ACS OMEGA

Open Access

http://pubs.acs.org/journal/acsodf

Article

Tensile Strength Statistics and Fracture Mechanism of Ultrahigh Molecular Weight Polyethylene Fibers: On the Weibull Distribution

Jinyou Ding, Gonglin Chen, Wei Huang, Jinlong Cheng, Ting Li, Chunzu Cheng,* and Jigang Xu

Cite This: *ACS Omega* 2024, 9, 12984−12991

Read Online

ACCESS | Metrics & More | Article Recommendations

ABSTRACT: To study the distribution of ultrahigh molecular weight polyethylene fiber (UHMWPE) strength, three groups of UHMWPE fibers were spun by the gel spinning method, which was undrafted raw fibers (with high strain at break) and fibers with different prespinning and postspinning draw ratios. It is found that even when the strain at break (ε_b) > 46%, the tensile strength of the fiber still obeys the Weibull distribution. The draw ratio has a great influence on the distribution of fiber strength, especially the draw ratios of the spinneret in the prespinning process. It may be that different drafting processes affect the fracture mechanism of the fibers. This paper analyzes and discusses that and proves it by differential scanning calorimetry and the taut tie molecules (TTMs) fractions. The parameters of the Weibull distribution suggest the quality of the fiber. The Weibull modulus is closely related to the dispersion of the fiber properties and processing parameters. The characteristic strength is similar to the test average strength, which is more suitable for the judgment of fiber reliability in actual use. At the same time, the normality of the samples was tested by Kolmogorov−Smirnov, Shapiro−Wilk, Jarque−Bera test, and quantile−quantile (Q-Q) plots, and the strength distribution was visually displayed by the bell curve. The results show that the Gaussian distribution is not so suitable to describe the strength distribution of the stretched fiber compared to the Weibull distribution.

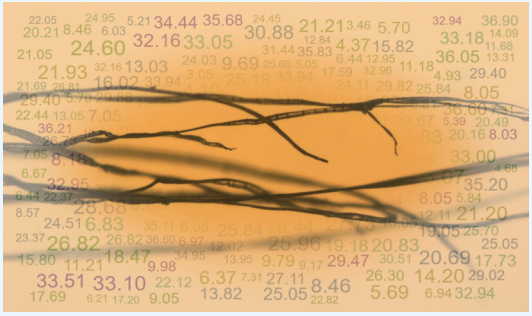

1. INTRODUCTION

Ultrahigh molecular weight polyethylene (UHMWPE) fiber has excellent mechanical properties and is the highest specific strength fiber at present. As early as the 1930s, some scholars studied the theoretical limit properties of polyethylene fiber. Studies have shown that the theoretical modulus of UHMWPE is 250−350 GPa,[1,2] and its theoretical strength can reach 20−60 GPa according to the molecular chain fracture mechanism. Since the 1970s, researchers have proposed a variety of preparation methods, including solid state extrusion,[3] surface growth,[4,5] ultrahigh stretching,[6,7] gel-spinning,[8,9] etc. The tensile strength of the fiber is constantly improving. The tensile strength in the actual test of UHMWPE reaches 6.4 GPa,[10] but this is far from the theoretical value.

In the structural model of UHMWPE fiber, microfibril consists of folded chain lamellae and amorphous regions,[11−14] and the fiber fracture process is controlled by molecular chain fracture and interchain slip.[15] For a long time, many molecular explanations have emerged for the fiber fracture process. Smook et al.[16,17] and Sun[18] et al. discussed the formation process of chain entanglement in fibers. They believed that during spinning, entanglement would be affected by external conditions, especially slip entanglement. During stretching, part of the entanglement would be opened, and chains would be removed from topological entanglement. Finally, the intermediate phase contains both topological entanglement and aggregation entanglement, but the amorphous region mainly contains topological entanglement. However, Balzano et al.[19] show that the crystalline phase has a discontinuous nature, entanglements are likely to be the cause of the interruption of the length of fibrillar crystals. In addition, studies[20,21] have shown that the number of entanglements is an important factor in the transformation of shish-kebab to shish crystal of fibers, which will affect the properties of fibers. These entanglements, chain ends, and kinks form defect areas in the fiber and cause microfibril breakage. However, Van Der Werff et al.[22] believe that the strain and fracture of existing UHMWPE fiber have not yet reached the degree of molecular chain fracture. Based on the microfibril model, it is proposed that the properties of fibers are affected by the content of taut tie molecules (TTMs) and the ratio of the length of the crystal region to the random region.

However, in any case, the ultrahigh strength of high-performance polyethylene fiber comes from its chemical

Received: November 23, 2023
Revised: February 3, 2024
Accepted: February 6, 2024
Published: March 5, 2024

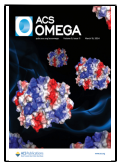

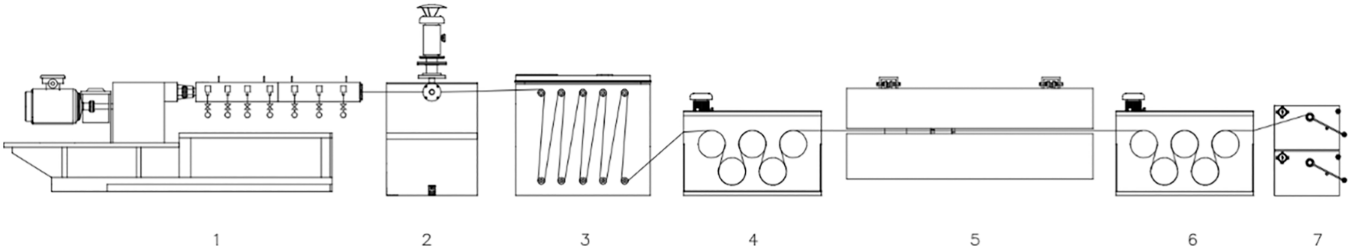

Figure 1. Prespinning process (1: twin-screw extruder, 2: metering pump and spinneret, 3: cooler bin, 4, 6: five-roller machine, 5: drying box, 7: winder).

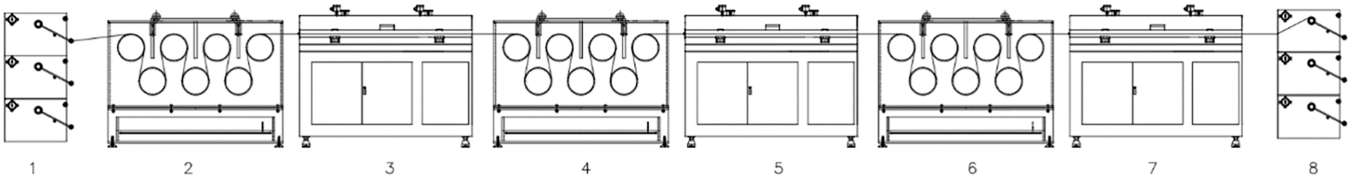

Figure 2. Postspinning process (1: unwinder, 2: guide roller, 3: first draft box, 4: first seven-roller machine, 5: second draft box, 6: second seven-roller machine, 7: third draft box,..., 8: winder)

Table 1. Process Parameters and Properties of All Fibers

group	number	prespinning draw ratios (λ_{ext}*λ_{pre})	postspinning draw ratios (λ_1*λ_2*λ_3)	total draw ratios	linear density (dtex)	tensile strength (cN/dtex)	tensile strength (GPa)	strain (%)
A	1	6*2.5		15	3554	2.02	0.19	46
	2	6*2		12	1896.8	2.69	0.26	71
B	3	22*1.2	5.2*1.3*1.1	196.3	76.68	24.72	2.35	4
	4	34*1.2	5.2*1.3*1.05	289.6	70.67	33.19	3.16	3
C	5	6*2	7*1.5*1.2	151.2	173.7	29.04	2.76	3
	6		8*1.5*1.2	172.8	141	32.54	3.09	3
	7		11*1.5*1.2	237.6	100	36.84	3.50	3

Table 2. Linear Fitting of Weibull Distribution of Fibers and Weibull Parameters

group	number	regression equation	correlation coefficient (R^2)	Weibull modulus	characteristic strength (cN/dtex)	average strength (cN/dtex)
A	1	$Y = -33.69 + 46.99x$	0.933	46.99	2.05	2.02
	2	$Y = -65.73 + 65.89x$	0.897	65.89	2.71	2.69
B	3	$Y = -37.59 + 11.59x$	0.986	11.59	25.62	24.51
	4	$Y = -55.11 + 15.58x$	0.825	15.58	34.37	33.2
C	5	$Y = -46.49 + 13.66x$	0.982	13.66	30.07	28.99
	6	$Y = -48.09 + 13.65x$	0.972	13.65	33.89	32.64
	7	$Y = -36.75 + 10.04x$	0.959	10.04	38.88	36.97

structure and regular molecular chain arrangement. From the phenomenological point of view, the fracture of fiber must occur at the "defect", which will become the "weakest link" of fiber fracture. The strain of UHMWPE fiber (ε_b) is less than 10%, which is consistent with the characteristics of brittle materials.[23] Weibull distribution was originally used for life analysis of brittle materials, such as ceramics,[24] carbon fiber,[25] and alloy materials.[26] At present, many studies have extended the application of Weibull distribution to natural fiber materials, such as wool,[27] spider silks,[28] and plant fibers.[29] In the field of chemical fibers, Boiko et al.[23,30−32] used the Weibull model in several studies to analyze fiber, spinning solvent, sample types (monofilament or multifilament), and mechanical properties (strength, modulus, strain). The studies involved materials such as UHMWPE fiber, polyamide6, and polypropylene. In other papers, the researcher extended the Weibull distribution to the self-bonding strength analysis of amorphous poly(ethylene terephthalate) (PET)[33] and amorphous polystyrene (PS).[34] To help understand the mechanisms of the self-healing interface. Schwartz et al.[35] also studied the influence of strain rate and gauge length on fiber properties based on the Weibull model, and their research made a great contribution to the application of the Weibull model in the field of UHMWPE.

With the support of the "weakest link" theory, we speculated that the UHMWPE fiber monofilaments with flexible macromolecular chains meet the Weibull distribution, which has been proved by Boiko et al.,[31,32] but it does not mean that the fiber bundles will also meet the Weibull distribution.[36,37] This is important, especially when the filament bundle is the main application.

In this paper, seven UHMWPE fibers with different properties were prepared by gel-spinning. Whether the tensile strength meets Weibull distribution was verified under different spinning drafts ratios, multistage drafts ratios, and strain (ε_b) > 10%. The Weibull distribution is based on the

https://doi.org/10.1021/acsomega.3c09230
ACS Omega 2024, 9, 12984−12991

"weakest link" theory.[38] If the strength distribution of the fiber conforms to the Weibull function, it means that its fracture is affected by random defects,[39] which may be surface cracks,[31] interface defects,[30,34] chain entanglement, and end points.[16] In addition, for brittle materials, on the one hand, fracture is difficult to predict, and crack propagation rarely occurs; on the other hand, the strength of fiber materials is very discrete, and unexpected fractures are easy to occur when the average value is used to describe the strength properties of the fiber. Therefore, another aim of this article is to propose a method to describe the strength properties of fibers and their reliability. At the same time, it links the molecular and phenomenological explanations of the fiber fracture process from a statistical point of view.

2. MATERIALS AND METHODS

2.1. Materials. UHMWPE ascent powder (Mw = 6×10^6 g/mol) purchased from Shanghai Lianle Chemical Technology Co., Ltd.). The solvent was decalin (*cis-trans* ratio 2:8, purchased from Jiangsu Middle Energy Technology Co., Ltd.).

2.2. Preparation of UHMWPE Fiber Samples. Figure 1 shows the prespinning process in the experiment. In this process, the UHMWPE powder (6 wt %) is fully swollen in decalin. Then the mixture was fed to the twin-screw extruder to dissolve completely. The product is extruded by the metering pump through the spinneret, cooled, and draw-down (λ_{ext}) to obtain gel-fiber, and then the gel-fiber was fed to the drying box for predrawing (λ_{pre}) and drying (80−100 °C), and finally, the dry raw fiber was obtained.

Figure 2 shows the postspinning process (multistage drafting) in the experiment. During the postspinning process, the raw fiber went through a guide roller, the first draft box, and the first seven-roller machine. The filaments were draw-down (λ_1) due to the difference in speed between the guide roller and the first seven-roller machine. Then the filaments were drawn in the second draft box between the first and second seven-roller machines (λ_2), in the third draft box between the third seven-roller machine and.....(λ_3), and even more. Finally, the fiber was fed into the winding machine for performance testing. The drafting temperature at all stages is within the range of 135 °C-145 °C. After postspinning drawing, the performance of the fiber is greatly improved. The process conditions are shown in Table 1.

The experiment was divided into three groups. In group A, in order to analyze the effect of strain, the fibers were dried raw fiber, that is, fibers that had not been postspinning drawing (No. 1 was dried twice, the second time was dried at 120 °C, and draw ratios was 2.5). In group B, in order to analyze the effect of the draw ratio of the spinneret in the prespinning process, the fibers had different draw ratios of the λ_{ext}. In group C, the purpose is to analyze the influence of multistage draw ratios in postspinning, which is different for fibers.

2.3. Characterization of UHMWPE Samples. Tensile strength was tested by an Instron 3343 tensile tester (USA). The fibers (70 untwisted monofilaments) were carefully wrapped around a dedicated cross head by the operator to avoid breaking the fibers. The fiber initial gauge length was 500 mm (group A initial gauge length was 250 mm, because the elongation of group A is particularly high and exceeds the range of the test equipment), and the fiber was stretched at a constant speed of 250 mm/min. Each fiber bundle was tested 30 times, and the average value of tensile strength was taken ($\bar{\sigma}$).

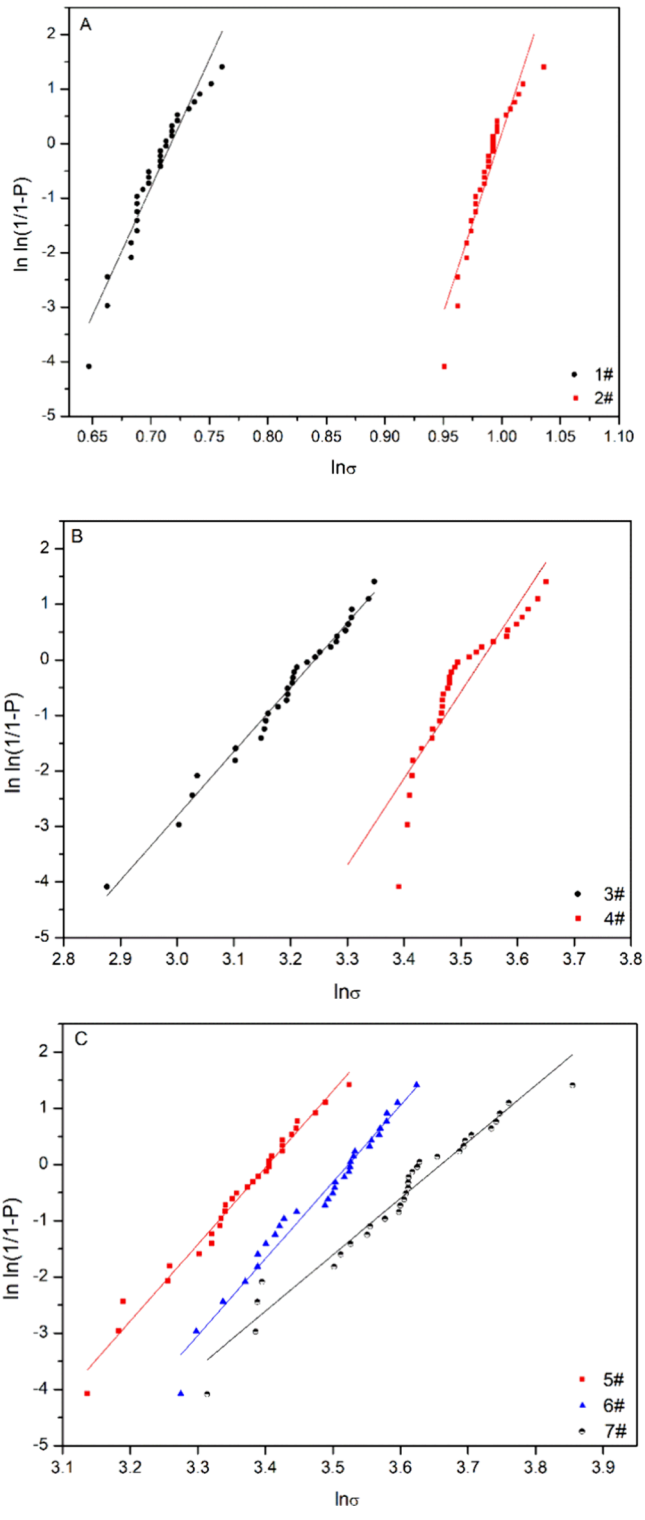

Figure 3. Weibull plots and linear fitting of all fiber strength test values ln σ_0 and ln ln 1/ (1 − P) (A: No. 1 and No. 2, B: No. 3 and No. 4, C: No. 5, No. 6, and No. 7).

The DSC thermograms were measured by using a Perkin−Elmer 8000 DSC differential scanning calorimeter at a heating rate of 20 °C/min in a nitrogen atmosphere. An indium standard was used for temperature calibration with an empty sample pan as the reference. The samples (1−2 mg) were heated from 30 to 175 °C.

https://doi.org/10.1021/acsomega.3c09230
ACS Omega 2024, 9, 12984−12991

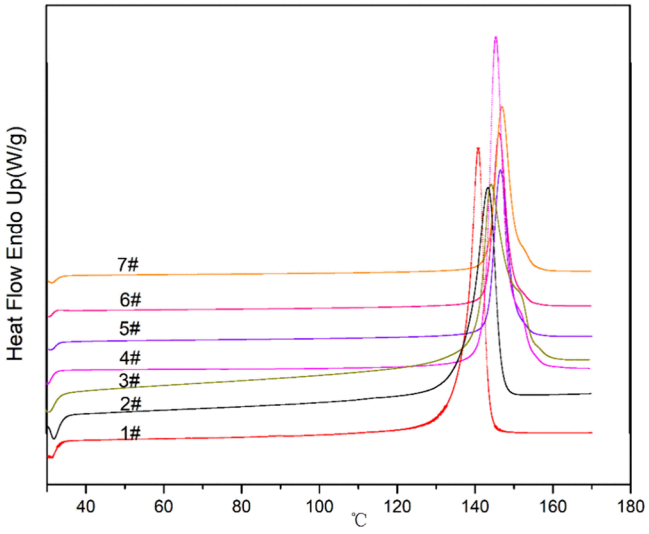

Figure 4. DSC thermograms of the fibers.

Table 3. Melting Point, Melting Enthalpy, Crystallinity, and TTM Fraction (β) of Fibers

group	number	melting point (°C)	melting enthalpy (g/J)	crystallinity (%)	TTM fraction (%)
A	1	140.84	223.19	76.17%	0.519
	2	143.18	215.24	73.46%	0.539
B	3	144.39	225.39	76.92%	7.113
	4	145.56	245.11	83.65%	9.348
C	5	146.16	251.75	85.92%	6.132
	6	146.08	258.86	88.34%	7.004
	7	146.82	271.55	92.67%	5.368

The crystallinity (X_c) of the UHMWPE sample after etching is calculated in eq 1.

$$X_c = \frac{\Delta H_m}{\Delta H_m^0} \times 100\% \quad (1)$$

The value of ΔH_m^0 is the melting enthalpy for 100% crystalline UHMWPE, which is assigned as 293 J/g.[40] The value of ΔH_m is the melting enthalpy for the sample, which was tested by DSC.

During the stretching process of the gel-fiber, crystals are broken to form microcrystals, and at the same time, tie molecules (TMs) are transformed into taut tie molecules (TTMs) with continuous stretching. According to the theory of Pennings et al.,[41] fiber tensile strength and modulus are positively correlated with the content of TTMs. The TTMs content indicates the dynamic change of the crystal. The TTM fraction (β) was calculated in eq 2.[2,41]

$$E = E_c \times \left(\frac{1 + \frac{1-x}{x-\beta}}{1 + \frac{1}{\beta} \times \frac{1-x}{x-\beta}} \right) \quad (2)$$

where E represents the modulus of the fiber that is found in tensile testing (1 cN/dtex = 0.09506 GPa), E_c represents the theoretical modulus of UHMWPE, the value is 350 GPa, and x represents the crystallinity (derived from DSC).

2.4. Weibull Distribution. The cumulative distribution function (CDF) of the Weibull distribution is shown in eq 3,

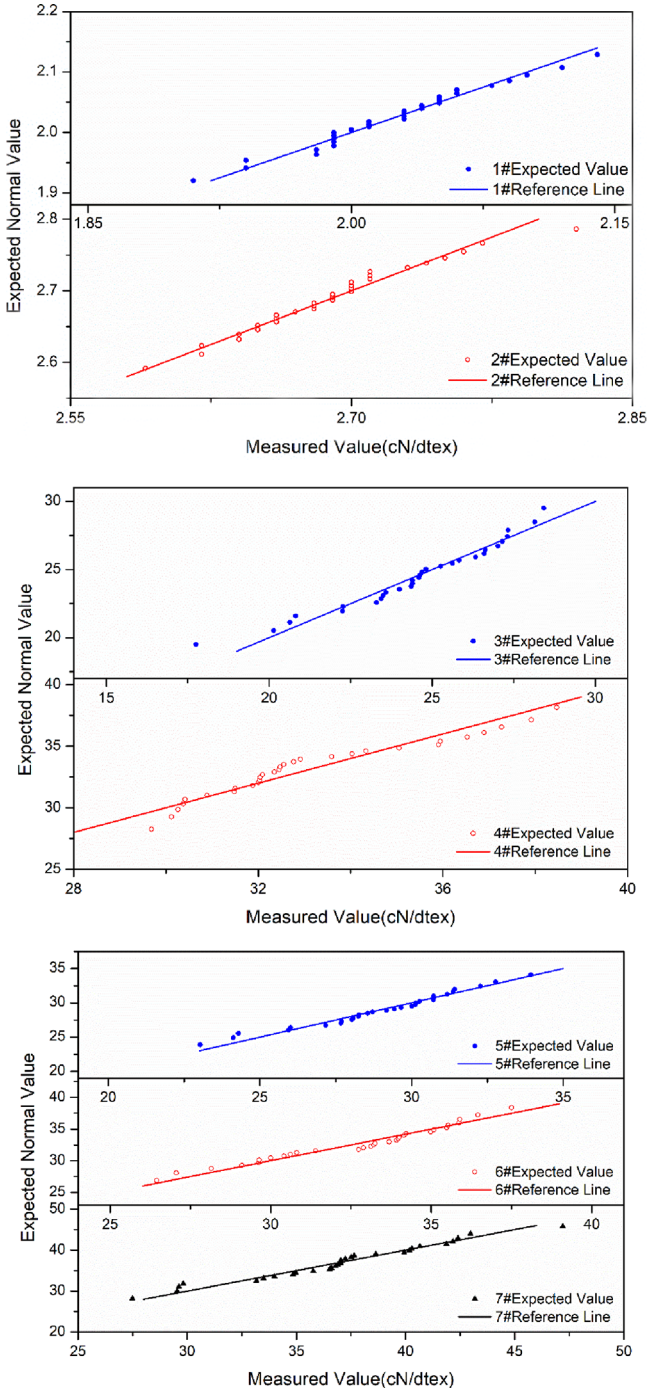

Figure 5. Quantile−quantile (Q-Q) plots of the fibers.

which must be satisfied if the tensile strength obeys the Weibull distribution.

$$P(\sigma) = 1 - e^{-(\sigma/\sigma_0)^m} \quad (3)$$

$P(\sigma)$ indicates the probability that the tensile strength is not higher than σ. σ is the test value of the tensile strength. σ_0 is the scaling parameter of the Weibull distribution, also known as the characteristic strength. m is the shape parameter of the Weibull parameter, also known as the Weibull modulus.

After double logarithmic transformation of the left and right sides of eq 3, we obtained eq 4.

https://doi.org/10.1021/acsomega.3c09230
ACS Omega 2024, 9, 12984−12991

Table 4. Statistical Parameters of the Strength Estimated in Several Normality Tests[a]

		test type						
		Kolmogorov−Smirnov		Shapiro−Wilk		Jarque−Bera	Q-Q	
group	number	statistic	*p*-value	statistic	*p*-value	*p*-value	standard deviation (cN/dtex)	average value (cN/dtex)
A	1	0.098	0.653	0.981	0.863	0.978	0.052	2.02
	2	0.133	0.190	0.977	0.742	0.510	0.049	2.69
B	3	0.114	0.414	0.956	0.241	0.287	2.505	24.51
	4	0.181	0.014*	0.923	0.032*	0.274	2.481	33.20
C	5	0.103	0.573	0.971	0.577	0.563	2.561	28.99
	6	0.147	0.096	0.957	0.252	0.437	2.878	32.64
	7	0.125	0.268	0.971	0.570	0.957	4.412	36.98

[a]"*" means "reject normality".

$$\ln \ln \frac{1}{1 - P(\sigma)} = m\ln \sigma - m\ln \sigma_0 \quad (4)$$

If we define $y = \ln \ln \frac{1}{1-P(\sigma)}$, $x = \ln \sigma$, $a = m$, $b = -m \ln \sigma_0$, we obtain a linear expression $y = ax + b$. It is clearly represented in a coordinate system.

Therefore, the test values of tensile strength are arranged in order from smallest to largest, that is, $\sigma_1 \leq \sigma_2 \leq \sigma_3 \leq \ldots\ldots \leq \sigma_N$.

The probability of the fiber breaking at a strength less than σ_i ($P(\sigma_i)$) can be expressed in eq 5.[32]

$$P(\sigma_i) = (i - 0.5)/N \quad (5)$$

σ_i represents the value ranked "i" in the sequence, N represents the total number of tensile strength test values.

The scatter plots of $\ln \ln 1/(1 - P)$ and $\ln\sigma$ are drawn on the coordinate axes. If the data points show a linear relationship, it indicates that the tensile strength of the fiber follows the Weibull statistics, and the regression equation is obtained by fitting the linear regression method. The slope is a shape parameter, and the scaling parameter σ_0 is obtained by solving eq 4. The fitting equations and Weibull parameters of the experiment are listed in Table 2.

3. RESULTS AND DISCUSSION

3.1. Analysis of Strain. The fibers in group A were without postspinning process. Table 1 shows the process parameters and properties of all fibers. It can be seen that the strain of group A fibers was high (No. 1, ε_b = 46.24%; No. 2, ε_b = 70.51%), and the strength is extremely low. Figure 3 shows the scatter plot and linear fitting of all fiber strength test values $\ln\sigma_0$ and $\ln 1/(1 - P)$. It can be seen from Figure 3a and Table 2 that although the breaking elongation of the group A fibers was high, the data distribution in the Weibull plot is basically close to a straight line, which indicates that the strength data of fibers conform to Weibull statistics. Therefore, we believe that the breakage of the fiber is caused by random "defects" (entanglement, chain ends, etc.) in the structure of the molecular chain. The correlation coefficient (R^2) of the fitting equation for group A fiber is small, especially for fiber No. 2. In the part with higher tensile strength, the data deviate greatly from the theoretical value. We believe that this may be due to the relative slip of molecular chains in the fracture process of group A fibers.[22] This results in the transfer of defects that occur randomly,[42] and uneven distribution as the molecular chain slips. This relative slip of the molecular chain is more likely to occur at a strength of 1/10 of the theoretical modulus,[43] which explains the anomaly in fiber No. 2.

The Weibull modulus (m) of No. 2 fiber was high, which indicates that the dispersion of fiber tensile strength was small, and the reliability of fiber quality was good. This may be related to the smaller draw ratio. It can be seen from Table 2 that the fibers with better fitting are consistent with this conclusion, which is also consistent with our general cognition.

Figure 4 shows the DSC thermograms of the fiber, and Table 3 shows the melting point (T_m), melting enthalpy (ΔH_m), crystallinity (X_c), and TTMs fraction (β) calculated according to the spectrum data. Curiously, it can be seen from Figure 3 and Table 3 that the T_m values of the two fibers in group A are quite different. Fiber No. 1 has a lower T_m (No. 1, T_m = 140 °C; No. 2, T_m = 143 °C,), but it has a higher crystallinity (No. 1, X_c = 76.17%; No. 2, X_c = 73.46%), which has also been observed in previous experiments.[44] This is due to the presence of solvent in the No. 1 fiber before secondary drying. During the secondary drying, solvation crystallization was produced under the action of a high temperature and solvent. After drying and drawing, part of the crystallization was transformed into the shish-kebab structure. This also resulted in a partial unraveling of the TTMs, thus showing a decrease of β in Table 3.

If TTMs are also regarded as a "defect", we assume that TTMs are randomly distributed in the fiber. It can be inferred that the higher the TTM fraction, the more evenly dispersed TTMs are in the fiber, the smaller the strength dispersion of the fiber, and the higher the Weibull modulus. The data in Tables 2 and 3 support this inference. However, it should be noted that the Weibull modulus is not completely controlled by TTMs, so in some cases, the Weibull modulus values do not show a strict proportional relationship with the TTM fraction.

3.2. Analysis of the Draw Ratio of Spinneret. Group B experiments were conducted to analyze the influence of the spinneret ratio (λ_{ext}). It can be seen from Figure 3b and Table 2 that the fiber tensile strength obtained by different λ_{ext} has different performances in the Weibull distribution. The collinearity of the tensile strength data of the No. 4 fiber is poor after processing, and the R^2 of the fitting equation is 0.825. This is due to the excessive spinneret draw ratio of No. 4 fiber, and the high nozzle stretch will lead to the fiber unwinding mainly by sliding unwinding, and at the same time, the entanglement will form irreversible defects.[18] Thus, in Weibull statistics of the strength data, these defects cause the test values to deviate from theory, which is consistent with the phenomenon in Figure 3b. In addition, a higher tensile ratio will also increase its TTMs fraction.[2]

In the DSC test spectrum in Figure 3 and Table 3, the fibers of the group B experiment showed a weak melting peak in the

https://doi.org/10.1021/acsomega.3c09230
ACS Omega 2024, 9, 12984−12991

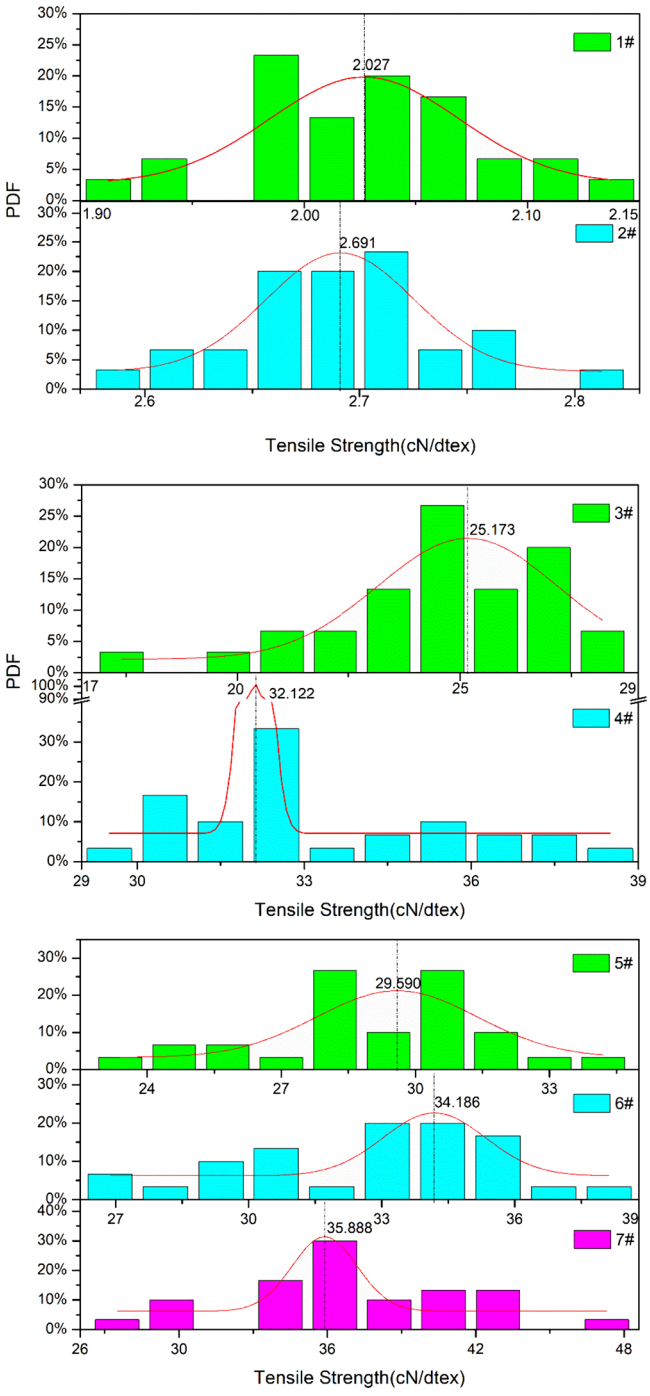

Figure 6. Histograms of the probability density function (PDF) and their corresponding Gaussian distribution of the fibers.

range of 150−155 °C, which reflected the transformation from orthogonal to hexagonal crystals and was the result of high multistage draw ratios.[44−46] After high extension drafting, the elongation chain component of the fiber is increased and the X_c and T_m of the fiber are increased. Fiber No. 3 has a relatively low draw ratio, its crystal is not perfect, reflecting a large peak width on the spectrum.

It is worth noting that in all three sets of tests, the Weibull characteristic strength (σ_0) is still close to the test mean value, which indicates that σ_0 is physically meaningful. As statistical data, they are more suitable for reliability indicators in actual use than the tensile strength test mean.

3.3. Analysis of the Draw Ratio of Postspinning. Group C experiments were conducted to analyze the influence of the postspinning draw ratio. As can be seen from Figure 3c and Table 2, the tensile strength value of group C fibers showed good collinearity in the Weibull plots, and the curve can be well-fitted (No. 5, R^2 = 0.982, No. 6, R^2 = 0.972, No. 7, R^2 = 0.959). This fully shows that the fracture mechanism of the fiber is in accordance with the defect random principle in this process. But we also found that the Weibull modulus was different under different postspinning processes. This indicates that the Weibull modulus is very sensitive to the properties of the fibers. On the whole, it shows that the higher the postspinning draw ratio, the lower the Weibull modulus, and the higher the dispersion of fiber properties. This trend is consistent with the fiber X_c and T_m shown in Table 3. The TTMs fraction begins to decrease after reaching the peak, because the high tensile stress causes TTM to open and crystallize. It can be seen from Table 3 that the crystallinity of the fiber reaches 92.67%.

3.4. Normality Analysis of All Fibers. Another common tool in the statistical method of fiber strength is the Gaussian distribution, which is followed by the strength statistics of many bundles of fibers. If the fiber fracture strength conforms to the Gaussian distribution, then it shows that the fiber fracture is controlled by the addition of multiple factors with the same weight.

We constructed the quantile−quantile (Q-Q) plots (Figure 5), and Kolmogorov−Smirnov, Shapiro−Wilk, and Jarque−Bera tests were used to test the normality of the seven fibers. Table 4 shows the parameters of several fibers in the normality test. It can be seen from Table 4 that Kolmogorov−Smirnov and Shapiro−Wilk tests show that fiber No. 4 has no normality and the collinearity of this fiber is poor in the Q-Q plots. However, the Jarque−Bera test combined with the skewness coefficient and kurtosis coefficient found that all 7 fibers had normality.

Figure 6 shows the histograms of the probability density function (PDF) of all fibers and their corresponding Gaussian distribution. As can be seen from the figure, the fitting curve of the group A fibers (undrawn) conforms to the typical "bell curve", which indicates that the strength of the unstretched fibers conforms to the Gaussian distribution. However, the curves fitted by the data of groups B and C (after drafting at different ratios) have different degrees of deviation. We do not know the reason for the above phenomenon at present, but it still indicates that the Gaussian distribution is not suitable to describe the strength of the fiber after drafting.

4. CONCLUSIONS

In this paper, we prepared 7 kinds of fibers by gel spinning method, and they were divided into three groups, unstretched raw fibers (group A), fibers with different prespinning drawn ratios (group B), and A2 fibers with different postspinning drawn ratios (group C). These groups represent several major stages of the fiber in the gel spinning process. We tested the tensile strength of these fibers 30 times and tried to describe them in terms of the Weibull distribution.

For the first time, we found that the breaking strength of unstretched fibers (group A) still conforms to the Weibull distribution, despite the elongation at break being greater than 46%. The influence of prespinning and postspinning on the strength distribution of the stretched fibers is discussed. Both of them are consistent with the Weibull distribution. This

https://doi.org/10.1021/acsomega.3c09230
ACS Omega 2024, 9, 12984−12991

shows that the strength of UHMWPE fibers follows a Weibull distribution regardless of the step in the fiber production process (fibers that are undrawn and different draft ratios).

The characteristic strength of the Weibull distribution is very close to the test average value of fiber strength, which indicates that the characteristic strength of the Weibull distribution has a physical significance. In addition, there is a huge difference in the Weibull modulus (group A, m = 46−96; groups B and C, m = 10−16) from the point of view of whether the fiber has been through the postspinning process. From the point of view of the drawn ratio (between groups or within groups), the Weibull characteristic strength and Weibull modulus undergo obvious changes. This shows that the change of the gel spinning process has a significant effect on the Weibull model. Since the Weibull distribution is a statistical model, the change of Weibull modulus combined with Weibull strength can well indicate the reliability of fiber strength in practical application, to avoid unexpected fiber breakage.

There are many molecular explanations for the theory of fiber fracture, but they have not been proven experimentally. Based on the analysis of the fiber's crystal degree and TTM fraction, and combined with the currently accepted theory, we guess that the fiber failure process includes the molecular chain fracture and relative slip to explain the behavior of these fibers in the Weibull model. It should be clarified that the Weibull distribution, as a statistical model, can only help us understand the molecular explanation of fiber breakage from a phenomenological point of view.

We also tested the normality of several fibers and verified their distribution in the Gaussian model. The bell-shaped curve fitted by group A fibers was consistent with the typical Gaussian distribution, while the drafted fibers (groups B and C) were not so suitable for the Gaussian distribution.

AUTHOR INFORMATION

Corresponding Author

Chunzu Cheng − *State Key Laboratory of Biobased Fiber Manufacturing Technology, China Textile Academy, Beijing 100025, China*; Email: chengchunzu@cta.gt.cn

Authors

Jinyou Ding − *State Key Laboratory of Biobased Fiber Manufacturing Technology, China Textile Academy, Beijing 100025, China*; orcid.org/0000-0001-7682-3466

Gonglin Chen − *State Key Laboratory of Biobased Fiber Manufacturing Technology, China Textile Academy, Beijing 100025, China*

Wei Huang − *State Key Laboratory of Biobased Fiber Manufacturing Technology, China Textile Academy, Beijing 100025, China*

Jinlong Cheng − *State Key Laboratory of Biobased Fiber Manufacturing Technology, China Textile Academy, Beijing 100025, China*

Ting Li − *State Key Laboratory of Biobased Fiber Manufacturing Technology, China Textile Academy, Beijing 100025, China*

Jigang Xu − *State Key Laboratory of Biobased Fiber Manufacturing Technology, China Textile Academy, Beijing 100025, China*

Complete contact information is available at: https://pubs.acs.org/10.1021/acsomega.3c09230

Notes

The authors declare no competing financial interest.

ACKNOWLEDGMENTS

The authors thank CTA (Tianjin) Science and Technology Development Co., Ltd. for its help in gel spinning equipment. The anonymous reviewers have also contributed considerably to the publication of this paper. In addition, I would like to thank the anonymous reviewers who have helped to improve the paper. This research did not receive any specific grant from funding agencies in the public, commercial, or not-for-profit sectors.

REFERENCES

(1) Smith, P.; Lemstra, P. J. Tensile strength of highly oriented polyethylene. *J. Polym. Sci., Polym. Phys. Ed.* **1981**, *19*, 1007−1009.

(2) Sun, Y.; Wang, Q.; Li, X.; et al. Investigation on dry spinning process of ultrahigh molecular weight polyethylene/decalin solution. *J. Appl. Polym. Sci.* **2005**, *98*, 474−483.

(3) Southern, J.; Porter, R. Polyethylene crystallized under the orientation and pressure of a pressure capillary viscometer. *Part I. Journal of Macromolecular Science, Part B* **1970**, *4*, 541−555.

(4) Hill, M. J.; Barham, P. J.; Keller, A. On the hairdressing of shish-kebabs. *Colloid Polym. Sci.* **1980**, *258*, 1023−1037.

(5) Pennings, A. J.; Torfs, J. Longitudinal growth of polymer crystals from flowing solutions 0.6. melting behavior of continuous fibrillar polyethylene crystals. *Colloid Polym. Sci.* **1979**, *257*, 547−549.

(6) Capaccio, G.; Ward, I. M. Preparation of ultra-high modulus linear polyethylenes; effect of molecular weight and molecular weight distribution on drawing behaviour and mechanical properties. *Polymer* **1974**, *15*, 233−238.

(7) Wu, W.; Black, W. B. High-strength polyethylene. *Polym. Eng. Sci.* **1979**, *19*, 1163−1169.

(8) Smith, P.; Lemstra, P. J. Ultrahigh-strength polyethylene filaments by solution spinning/drawing. *J. Mater. Sci.* **1980**, *15*, 505−514.

(9) Smith, P.; Lemstra, P. J.; Kalb, B.; et al. Ultrahigh-strength polyethylene filaments by solution spinning and hot drawing. *Polym. Bull.* **1979**, *1*, 733−736.

(10) Yeh, J.; Wang, C.; Yu, W.; et al. Ultra-drawing and ultimate tensile properties of ultrahigh molecular weight poly-ethylene composite fibers filled with functionalized nano-alumina fillers. *Polym. Eng. Sci.* **2015**, *55*, 2205−2214.

(11) Peterlin, A. Molecular model of drawing polyethylene and polypropylene. *J. Mater. Sci.* **1971**, *6*, 490−508.

(12) Nalankilli, G. Gel spinning - a promising technique for the production of high performance fibres. *Man-Made Text. India* **1997**, *40*, 237−242.

(13) Tian, Y.; Zhu, C.; Gong, J.; et al. Transition from shish-kebab to fibrillar crystals during ultra-high hot stretching of ultra-high molecular weight polyethylene fibers: In situ small and wide angle X-ray scattering studies. *Eur. Polym. J.* **2015**, *73*, 127−136.

(14) Zheng, X. Y.; Yu, J. R.; Liu, Z. F. Research on the technique of gel spinning. *Hi-Tech Fiber Appl.* **2000**, *25*, 29−34.

(15) Bastiaansen, C. W. M. Tensile strength of solution-spun, ultra-drawn ultra-high molecular weight polyethylene fibres: 1. *Influence of fibre diameter, Polymer* **1992**, *33*, 1649−52.

(16) Smook, J.; Hamersma, W.; Pennings, A. J. The fracture process of ultra-high strength polyethylene fibres. *J. Mater. Sci.* **1984**, *19*, 1359−1373.

(17) Smook, J.; Pennings, J. Influence of draw ratio on morphological and structural changes in hot-drawing of UHMW polyethylene fibres as revealed by DSC. *Colloid Polym. Sci.* **1984**, *262*, 712−722.

(18) Sun, Y.; Duan, Y.; Chen, X.; et al. Research on the molecular entanglement and disentanglement in the dry spinning process of UHMWPE/decalin solution. *J. Appl. Polym. Sci.* **2006**, *102*, 864−875.

(19) Balzano, L.; Coussens, B.; Engels, T.; et al. Multiscale structure and microscopic deformation mechanisms of gel-spun ultrahigh-molecular-weight polyethylene fibers. *Macromolecules* **2019**, *52*, 5207−16.
(20) An, M.; Xu, H.; Lv, Y.; et al. Structural difference of gel-spun ultra-high molecular weight polyethylene fibers affected by cold drawing process. *Fibers Polym.* **2017**, *18*, 549−554.
(21) Wang, H.; Liu, R.; Yu, J.; et al. Effect of Gel-spun solution concentration on the structure and properties of UHMWPE monofilaments with coarse denier. *Fibers Polym.* **2022**, *23*, 1807−1816.
(22) Van Der Werff, H.; Pennings, A. J. Tensile deformation of high strength and high modulus polyethylene fibers. *Colloid Polym. Sci.* **1991**, *269*, 747−763.
(23) Boiko, Y. M.; Marikhin, V. A.; Myasnikova, L. P.; et al. Statistical viscoelastic and fracture mechanical properties of gel-cast ultra-oriented high-strength film threads of ultra-high-molecular-weight polyethylene. *Colloid Polym. Sci.* **2018**, *296*, 1651−1656.
(24) ASTM Standard practice for reporting uniaxial strength data and estimating Weibull distribution parameters for advanced ceramics. *1998 Annual Book of ASTM Standards* 2007 ASTM International (ASTM C1239−13, 2018).
(25) Deng, F.; Lu, W.; Zhao, H.; et al. The properties of dry-spun carbon nanotube fibers and their interfacial shear strength in an epoxy composite. *Carbon* **2011**, *49*, 1752−1757.
(26) Yang, C.; Jiang, S. Weibull statistical analysis of strength fluctuation for failure prediction and structural durability of friction stir welded Al−Cu dissimilar joints correlated to metallurgical bonded characteristics. *Materials* **2019**, *12*, 205.
(27) Moradi, S.; Liu, X.; Najar, S. S.; et al. Tensile strength prediction of irregular fibres using diameter-dependent Weibull analysis. *J. Text. Inst.* **2019**, *110*, 600−605.
(28) Greco, G.; Pugno, N. M. Mechanical properties and Weibull scaling laws of unknown spider silks. *Molecules* **2020**, *25*, 2938.
(29) Caren, K. J.; Kenneth, N. D.; David, M. M. Strength properties of surface-modified giant cavendish;(musa acuminata); Banana fibers. *Journal of Natural Fibers* **2022**, *19*, 12746−12759.
(30) Boiko, Y.; Marikhin, V.; Myasnikova, L. Statistical analysis of the mechanical behavior of high-performance polymers: Weibull's or gaussian distributions? *Polymers (Basel)* **2022**, *14*, 2841.
(31) Boiko, Y. M.; Marikhin, V. A.; Myasnikova, L. P. Tensile strength statistics of high-performance mono- and multifilament polymeric materials: On the validity of normality. *Polymers (Basel)* **2023**, *15*, 2529.
(32) Boiko, Y. M.; Marikhin, V. A.; Moskalyuk, O. A.; et al. Features of statistical strength distributions in mono- and polyfilament ultra-oriented high-strength fibers of ultrahigh-molecular-weight polyethylene. *Phys. Solid State* **2020**, *62*, 676−681.
(33) Boiko, Y. M. Impact of crystallization on the development of statistical self-bonding strength at initially amorphous polymer-polymer interfaces. *Polymers (Basel)* **2022**, *14*, 4519.
(34) Boiko, Y. M. Evolution of statistical strength during the contact of amorphous polymer specimens below the glass transition temperature: influence of chain length. *Materials (Basel)* **2023**, *16*, 491.
(35) Schwartz, P.; Netravali, A.; Sembach, S. Effects of strain rate and gauge length on the failure of ultra-high strength polyethylene fibers. *Text. Res. J.* **1986**, *56*, 502.
(36) Porwal, P. K.; Beyerlein, I. J.; Phoenix, S. L. Phoenix, Statistical strength of a twisted fiber bundle: An extension of daniels equal-load-sharing parallel bundle theory. *J. Mech. Mater. Struct.* **2006**, *1*, 1425−1447.
(37) Daniels, H. E. The statistical theory of the strength of bundles of threads. I. *Proc. R. Soc. London, Ser. A* **1945**, *183*, 405−435.
(38) Zok, F. W. On weakest link theory and Weibull statistics. *J. Am. Ceram. Soc.* **2017**, *100*, 1265−1268.
(39) Thomason, J. L. On the application of Weibull analysis to experimentally determined single fibre strength distributions. *Compos. Sci. Technol.* **2013**, *77*, 74−80.
(40) Hosseinnezhad, R.; Vozniak, I.; Romano, D.; et al. Formation of UHMWPE Nanofibers during solid-state deformation. *Nanomaterials* **2022**, *12*, 3825.
(41) Penning, J. P.; Van Der Werff, H.; Roukema, M.; et al. On the theoretical strength of gelspun/hotdrawn ultra-high molecular weight polyethylene fibres. *Polym. Bull.* **1990**, *23*, 347−352.
(42) Kalb, B.; Pennings, A. J. Maximum strength and drawing mechanism of hot drawn high molecular weight polyethylene. *J. Mater. Sci.* **1980**, *15*, 2584−2591.
(43) Asa, H. B.; Rodney, A.; Linda, S. S.; et al. On the tensile strength distribution of multiwalled carbon nanotubes. *Appl. Phys. Lett.* **2005**, *87*, 203106.
(44) Hoogsteen, W.; Brinke, G. T.; Pennings, A. J. DSC experiments on gel-spun polyethylene fibers. *Colloid Polym. Sci.* **1988**, *266*, 1003−1013.
(45) Hu, W.; Buzin, A.; Lin, J. S.; et al. Annealing behavior of gel-spun polyethylene fibers at temperatures lower than needed for significant shrinkage. *Journal of Polymer Science Part B* **2003**, *41*, 403−417.
(46) Wu, H.; Liao, T.; Zhu, B.; et al. Reversed thermal stability between stress-induced melting and recrystallized crystallites and original inclined ones in moderately stretched ultra-high molecular weight polyethylene and high density polyethylene. *Polymer* **2023**, *270*, No. 125799.

https://doi.org/10.1021/acsomega.3c09230
ACS Omega 2024, 9, 12984−12991